

# H-Shaped Resonant Optical Antennas with Slot Coupling

Xu Han · Xiang Ji · Hanqing Wen · Jiasen Zhang

Received: 18 April 2011 / Accepted: 28 July 2011 / Published online: 4 August 2011  
© Springer Science+Business Media, LLC 2011

**Abstract** H-shaped resonant optical antennas are proposed by adding resonant strips at the ends of arms of short dipole antennas. Numerical simulations using finite-difference time-domain method show that the H-shaped antennas present greater electric field enhancement compared with optical dipole antennas at the same resonant wavelength. The slot coupling between the two arms also results in a smaller full width at half maximum of the scattering spectra. Two field-enhancing mechanisms are found to decide the resonant properties of the H-shaped antennas. The influence of the geometry is studied.

**Keywords** Resonant optical antennas · Surface plasmons · Metal optics · Micro-optics

## Introduction

Recently, resonant antennas operated in optical frequency range have attracted great interest because of their promising abilities to interconvert propagating field and localized field as well as the field enhancement in the feed gap [1, 2]. The resonance decisively depends on the nature of antennas, which is dictated by the shape, material, dimensions of the antennas, and operation frequency. For this reason, optical antennas of different shapes, such as dipole antennas [1], bow-tie antennas [3], square spiral antennas [4], V-shaped antennas [5], Yagi-Uda antennas [6], sandwiched antennas [7], slot antennas [8], and L-shaped

antennas [9] have been proposed. Despite their distinguishing features, all of these antennas have demonstrated a localized and strongly enhanced field in the feed gap when they are properly engineered. Many applications have been demonstrated in the fields of biological and chemical sensors [10, 11], nonlinear spectroscopy [12, 13], and optoelectronic devices [14, 15]. Optical antennas were also used to enhance the spontaneous emission of a fluorescent dye by more than a factor of 5 [16]. The valuable properties of optical antennas originate from the resonance of surface plasmon polaritons in the antenna arms and the coupling between the two arms, which is usually limited to the feed gap. Unlike radiowave and microwave antennas, optical antennas usually are not driven with galvanic transmission lines. More complicated optical antennas, whose structures may be deviated evidently from that of their radiowave and microwave counterparts, can be designed in order to improve their resonant properties.

In this paper, we propose H-shaped resonant optical antennas to implement high electric field enhancement factors and narrow full widths at half maximum (FWHMs) of the scattering spectra. Besides the feed gap coupling, the two arms of the H-shaped antennas also couple like a plasmonic slot waveguide [17–19]. Numerical simulations using the finite-difference time-domain technique show that the field enhancement factor of the H-shaped antenna is twice as big as that of a dipole antenna at the same resonant wavelength. Meanwhile, the FWHM of the H-shaped antenna is about a half of that of the dipole antenna. These superior properties are attributed to the nature of the high-quality factor (Q factor) symmetric mode of the slot cavity. The field-enhancing mechanism and the geometrical influence on the resonant properties of the H-shaped antennas are studied.

---

X. Han · X. Ji · H. Wen · J. Zhang (✉)  
State Key Laboratory for Mesoscopic Physics and Department  
of Physics, Peking University,  
Beijing 100871, People's Republic of China  
e-mail: jszhang@pku.edu.cn

## H-shaped resonant optical antennas

The incident light gives rise to standing surface charge waves on the arms of the optical resonant dipole antennas. The reflectivity of the waves at the ends is usually fairly low, which results in a low Q factor as well as the field enhancement. Here, an H-shaped resonant optical antenna is formed by adding a short dipole antenna in the middle of a slot cavity. Due to the slot waveguide structure, the H-shaped resonant optical antenna, which is schematically shown in Fig. 1a, has a narrow FWHM and a high field enhancement. The short dipole antenna has a cross section of  $40 \times 40 \text{ nm}^2$ . Its arm length is labeled as  $l$ , and its feed gap is kept to be 20 nm. The thickness of the two strips is 40 nm, the same as that of the short dipole antenna. The length of each strip is labeled as  $L$  and the width  $W$ . In the simulations, the perfectly matched layer absorbing boundary conditions are implemented at the boundaries of the modeling region. All other surrounding space is supposed to be the vacuum. Because the feature size in the  $x$ -direction is smaller than those in the other two directions, the grid spacing along the  $x$ -direction is set to be 1 nm, while those along the  $y$ - and  $z$ -directions are set to be 2 nm. When a smaller mesh is used, the simulation results change slightly. The dielectric constants of gold are from Lynch et al. [20]. The H-shaped antenna is illuminated by an  $x$ -polarized light source from the top along the  $z$ -axis with amplitude of 1 V/m. Here, the vacuum resonant wavelength of the H-shaped antenna is adjusted to be  $\lambda_0 = 830 \text{ nm}$ , which is the typical wavelength of Ti-sapphire lasers, by adjusting the value of  $L$  for different  $l$  while  $W$  is fixed at 65 nm. The combinations of  $L$  and  $l$  are shown in the inset of Fig. 1b. The field enhancement factors at the center of the gap as well as FWHMs for different combinations of  $L$  and  $l$  are calculated, and the results are shown in Fig. 1b. It shows that the field enhancement factor increases with increasing  $l$  until it reaches the maximum when  $l$  is 35 nm. Then it gradually decreases toward the limit of  $L=0$ , where the H-shaped antenna becomes a dipole antenna. Nevertheless, the FWHM monotonically increases with increasing  $l$ . For  $l=35 \text{ nm}$  and  $L=320 \text{ nm}$ , the field enhancement factor of

the H-shaped antenna is 2,670, which is about twice that of a dipole antenna (1,287) with arm length 149 nm, feed gap 20 nm and a same cross section of  $40 \times 40 \text{ nm}^2$  at the resonant wavelength 830 nm. At the same time, the FWHM of the H-shaped antenna, 78 nm, is evidently smaller than that of the dipole antenna, 136 nm. This means that the H-shaped antenna has a higher Q factor, which can be equivalently defined as “resonant wavelength over FWHM.” The time-averaged near-field intensity distribution of  $|\mathbf{E}_x|^2$  for  $l=35 \text{ nm}$  and  $L=320 \text{ nm}$  in the  $z=0$  plane at the resonant wavelength of 830 nm is shown in Fig. 1c. It can be seen that the H-shaped antenna has a strong field concentration in the feed gap.

## The field-enhancing mechanism of H-shaped antennas

In order to analyze the resonant mechanism of the H-shaped antenna, resonant properties of the strips alone, without the short dipole antenna in the middle, are investigated. The coupled strips form the so-called slot cavity, which is schematically shown in Fig. 2a. It consists of two same gold strips with a thickness of 40 nm. The length of each strip is labeled as  $L$ , and the width  $W$ . Firstly, the size of each strip of the slot cavity is set as  $L=368 \text{ nm}$  and  $W=65 \text{ nm}$ . The separation distance between the two trips is set to be 20 nm. The scattering spectrum at the center of the slot cavity is calculated with an  $x$ -polarized incident beam, and the result is shown in Fig. 2b. It can be seen that the cavity has a resonant wavelength of 830 nm and an FWHM of about 60 nm, which is much smaller than that of optical dipole antennas. The time-averaged near-field intensity distributions of  $|\mathbf{E}_x|^2$  in the  $z=0$  plane at the resonant wavelength 830 nm are shown in Fig. 2c with a field enhancement factor of 230 at the center of the slot. A typical 2nd-order symmetric resonant mode [17] is observed in the slot cavity. When the separation distance is increased while other parameters are unchanged, the field enhancement factor decreases whereas the resonant wavelength keeps nearly invariant.

**Fig. 1** **a** Schematic of an H-shaped antenna. **b** Field enhancement factors and FWHMs at the center of the gap versus  $l$ . The inset:  $L$  versus  $l$  for the resonant wavelength 830 nm. **c** Near-field intensity distribution of  $|\mathbf{E}_x|^2$  for  $l=35 \text{ nm}$  and  $L=320 \text{ nm}$  in the  $z=0$  plane at the resonant wavelength of 830 nm. The dashed lines outline the boundaries of the antenna

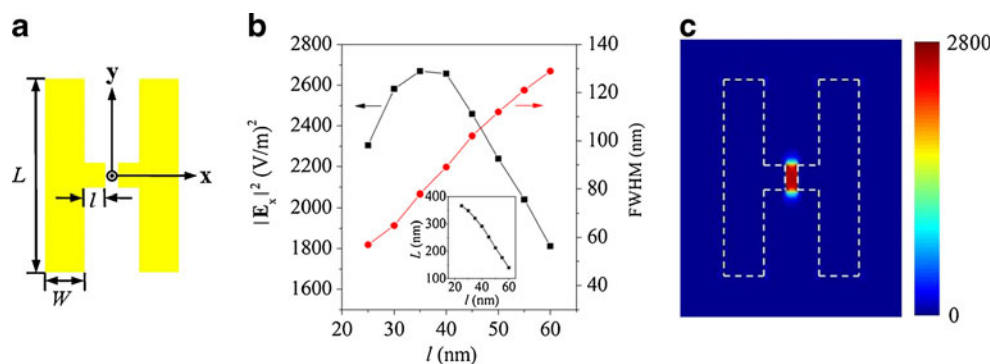
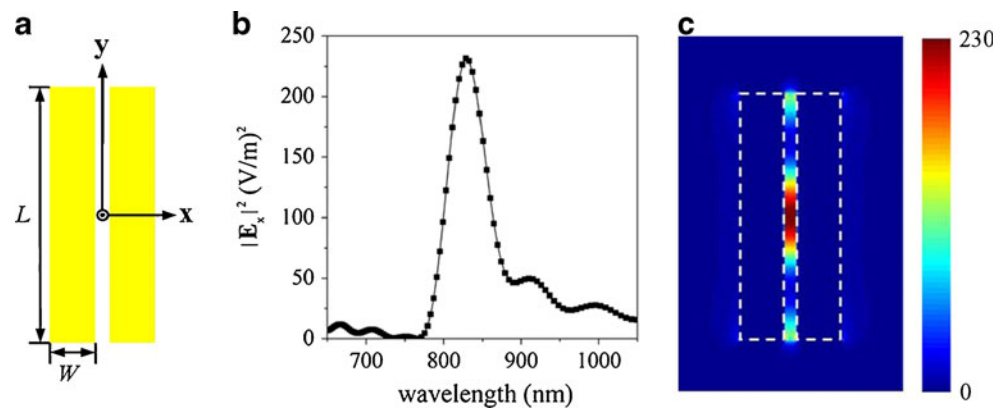


**Fig. 2** **a** Schematic of a slot cavity. **b** Scattering spectrum at the center of the slot cavity. **c** Near-field intensity distributions of  $|E_x|^2$  in the  $z=0$  plane at the incident wavelength 830 nm. The dashed lines outline the boundaries of the slot cavity



Then, the instantaneous electric current density vector distributions of both the slot cavity and the H-shaped antenna with the same resonant wavelength 830 nm are calculated. The maximum instantaneous electric current density distributions in the  $z=0$  plane are shown in Fig. 3. In the two gold strips of the slot cavity, typical standing waves are observed with the symmetric mode: one node appears in the middle for each strip. From Fig. 3a, it can be seen that most electric currents are perpendicular to the electric field vector of the incident light. According to the continuity equation, the charge density is proportional to the divergence of the current density vector for a monochromatic field. Therefore, more charges will pile up around the current nodes generating enhanced field at the center of the slot. This effect originates from the coupling between the two strips because electric currents in one single strip are mostly parallel to the electric vector of the incident beam rather than perpendicular to it. When a short dipole antenna is added in the middle of the slot, the two feed points of the dipole antenna become current nodes and the electric currents flow into the arms of the short dipole antenna, as shown in Fig. 3b. Accordingly, the short dipole antenna provides an influx concentration for electric currents, so

that charges pile up more compactly around the feed points of the H-shaped antenna resulting in further enhanced electric field in the feed gap. Moreover, the merit of high Q factor of the slot cavity mode makes the FWHM of the H-shaped antenna much smaller than that of a dipole antenna. Although most electric currents in the H-shaped antenna are parallel to the  $y$ -direction, no resonant behavior is found for a  $y$ -polarized incident light.

The arms of the dipole antenna can be considered as nanorod cavities, of which losses and Q factor are usually inferior to those of slot cavities due to the coupling between the two strips of the slot cavity. Therefore, in the case of the H-shaped antenna, extra coupling is induced by adding the slot cavity parts resulting in stronger resonant collective oscillations of the free electron gas, which generates greater field enhancement and smaller FWHM to overwhelm the dipole antenna.

### Influences of geometrical parameters and substrate

The influences of the geometric parameter  $W$  upon the resonance of both the slot cavities and the H-shaped antennas are investigated. For the slot cavity,  $L$  and the feed gap are kept to be 368 and 20 nm, respectively. The resonant wavelength of the slot cavity, which is shown in Fig. 4a, decreases monotonously when  $W$  increases from 40 to 100 nm. Nevertheless, the FWHM hardly changes (Fig. 4a). The field enhancement factor gradually increases with increasing  $W$  (Fig. 4b).

However, for the H-shaped antennas, the influence of  $W$  is different. Here, the values of  $l$ ,  $L$ , and feed gap are kept to be 35, 320, and 20 nm, respectively. When  $W$  is increased from 40 to 65 nm, the resonant wavelength blueshifts to reach a minimum of 830 nm. Meanwhile, the field enhancement factor increases to the maximum of 2,670 (Fig. 4b). As  $W$  continues to increase, the resonant wavelength then redshifts while the field enhancement factor gradually decreases. The FWHM monotonically

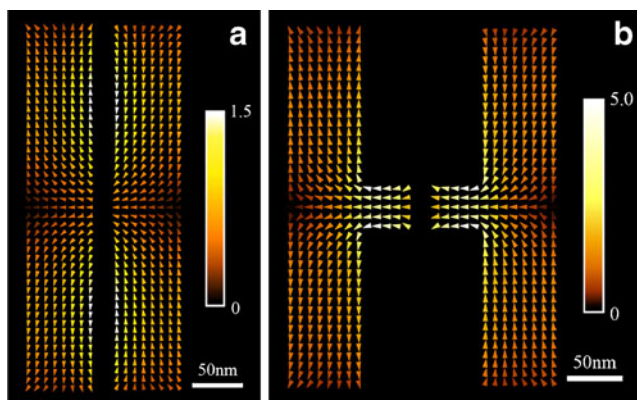


**Fig. 3** Maximum instantaneous electric current density distributions in the  $z=0$  plane of **a** the slot cavity and **b** the H-shaped antenna at the resonant wavelength 830 nm

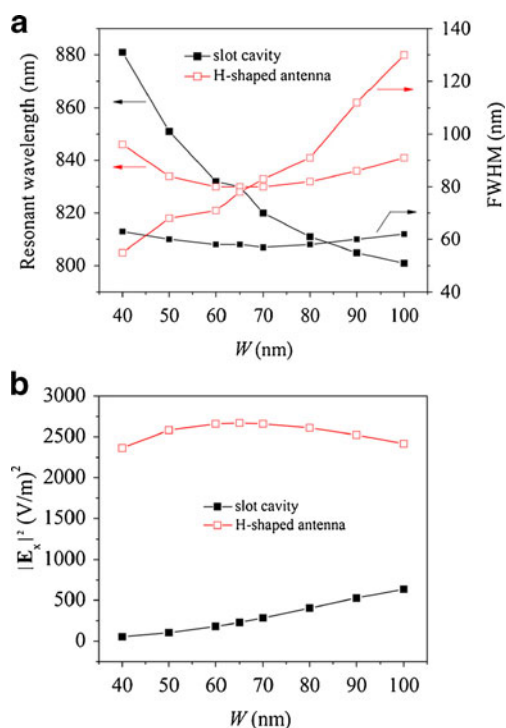


**Fig. 4** **a** Resonant wavelengths and FWHMs of the slot cavity and the H-shaped antenna versus  $W$ . **b** Field enhancement factors of the slot cavity and the H-shaped antenna versus  $W$

increases with increasing  $W$ . Therefore, the resonant properties of the H-shaped antennas depend on two kinds of mechanism. When  $W$  is small (from 40 to 65 nm), the slot coupling is relatively strong and acts as a predominate mechanism leading to the blueshift of the resonant wavelength. Further increase of  $W$  results in weaker slot coupling; meanwhile, the effect of the dipole antenna becomes more decisive leading to the redshift of the resonant wavelength. The dependence of enhancement factors of the slot cavities and the H-shaped antennas on  $W$ , which is shown in Fig. 4b, is also evidence of the two different kinds of mechanism that influence the resonant properties of the H-shaped antennas.

By increasing  $L$  of an H-shaped antenna, high-order resonant modes can be obtained. Figure 5 shows the time-averaged near-field intensity distribution of  $|E_x|^2$  in the  $z=0$  plane of an H-shaped antenna at the resonant wavelength 830 nm with  $l=35$  nm,  $W=65$  nm,  $L=868$  nm, and a 20-nm feed gap. The enhancement factor and FWHM are 694 and 46 nm, respectively. In the slot, two extra highlighted regions are observed, which present a 4th-order resonant mode similar to that in a slot cavity [21]. Although the 4th-order resonant H-shaped antenna has a lower enhancement factor, its FWHM is much smaller than that of the 2nd-order resonant H-shaped antenna.

Due to the coupling between the arms of the H-shaped antenna, its resonant properties are more sensi-

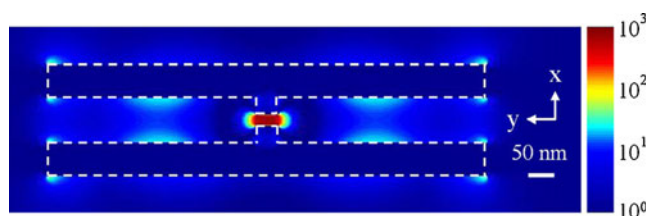


**Fig. 5** Near-field intensity distribution of  $|E_x|^2$  in the  $z=0$  plane for the 4th-order resonant mode of an H-shaped antenna at the resonant wavelength of 830 nm. The dashed lines outline the boundaries of the antenna

tive to the gap size than those of the dipole antenna. When the gap size is set to 10 nm (30 nm) and other parameters maintain  $l=35$  nm,  $W=65$  nm, and  $L=320$  nm, the field enhancement factor and the resonant wavelength of the H-shaped antenna become 9,007 and 920 nm (1,117 and 793 nm), respectively. The corresponding results of the dipole antenna with an arm length of 149 nm are 3,600 and 876 nm (660 and 807 nm).

In order to give more practical results, an underlying dielectric substrate is then added beneath the H-shaped antenna and the influence is studied. The substrate is supposed to infinitely stretch along  $\pm x$ ,  $\pm y$  and  $-z$  directions, which means that in our simulation, the substrate crosses the absorbing boundaries along those directions. Firstly, the material of the substrate is set to be glass with the refractive index of 1.5. The size of the H-shaped antenna is adjusted to be  $L=200$  nm,  $l=35$  nm, and  $W=60$  nm, when it presents the resonant wavelength of 830 nm and highest field enhancement. The scattering spectrum at the center of the H-shaped antenna is calculated as well as that of a dipole antenna with arm length of 118 nm placed on the same substrate for comparison. Although the H-shaped antenna still has a greater enhancement factor of 781 and a smaller FWHM of 117 nm than those of the dipole antenna (466 and 179 nm, respectively), the superiority of the H-shaped antenna diminishes. The presence of the substrate weakens the field

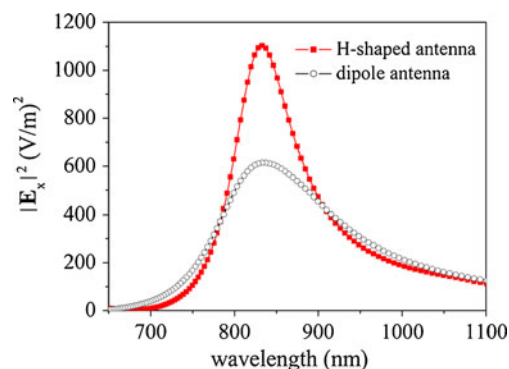


**Fig. 6** Scattering spectra at the centers of the H-shaped antenna and the dipole antenna when the refractive index of the substrate is 1.385



enhancement and broadens the resonant peak. This is because the dielectric substrate increases the energy dissipation. Therefore, a substrate with a lower index is preferable. Then, the material of the substrate is changed to  $\text{MgF}_2$  glass with a refractive index of 1.385. In order to be resonant at 830 nm, the size of the H-shaped antenna is set as  $L=232$  nm,  $l=35$  nm,  $W=56$  nm, and the arm length of the dipole antenna is 123 nm. In this case, the enhancement factor of the H-shaped antenna is 1,103 and the FWHM is 95 nm, while the dipole antenna presents an enhancement factor of 614 and an FWHM of 178 nm (shown in Fig. 6). The results indicate that the H-shaped antennas are a better choice in practical applications.

## Conclusions

In summary, we have proposed H-shaped resonant optical antennas, which present a great field enhancement with a desirable small FWHM. These preferable properties are attributed to the slot coupling between the two arms, which is a different enhancement mechanism from other kinds of optical resonant antennas. The nature of the symmetric mode of the slot cavity results in a reduced FWHM, and the short dipole antenna in the middle of the slot compactly concentrates charges generating greatly enhanced field. The geometrical dependence of the resonant properties shows that two mechanisms dominate the resonance of the H-shaped antennas. The field enhancement at the resonant wavelength is the result of the tradeoff between the two mechanisms: slot coupling and dipole antenna effect. Due to their superior properties, the H-shaped antennas can be expected to have many applications in nanophotonic and plasmonic devices, biosensors, and nonlinear spectroscopy.

**Acknowledgments** This work was supported by the National Natural Science Foundation of China under Grants 61036005 and 11074015, the Research Fund for the Doctoral Program of Higher Education under Grant 20090001110010, and the National Basic Research Program of China under Grant 2009CB623703.

## References

- Mühlschlegel P, Eisler H-J, Martin OJF, Hecht B, Pohl DW (2005) Resonant Optical Antennas. *Science* 308:1607–1609
- Bharadwaj P, Deutsch B, Novotny L (2009) Optical Antennas. *Adv Opt Photon* 1:438–483
- Fromm DP, Sundaramurthy A, Schuck PJ, Kino G, Moerner WE (2004) Gap-Dependent Optical Coupling of Single “Bowtie” Nanoantennas Resonant in the Visible. *Nano Lett* 4:957–961
- Alda J, Rico-García JM, López-Alonso JM, Boreman G (2005) Optical antennas for nano-photonic applications. *Nanotechnology* 16:S230–S234
- Yang J, Zhang J, Wu X, Gong Q (2007) Electric field enhancing properties of the V-shaped optical resonant antennas. *Opt Express* 15:16852–16859
- Hofmann HF, Kosako T, Kadoya Y (2007) Design parameters for a nano-optical Yagi-Uda antenna. *New J Phys* 9:217
- Wang L, Zhang J, Wu X, Yang J, Gong Q (2008) Resonances of sandwiched optical antenna. *Opt Commun* 281:5444–5447
- Kumar VD, Asakawa K (2009) Investigation of a slot nano-antenna in optical frequency range. *Photonics and Nanostructures-Fundamentals and Applications* 7:161–168
- Yang J, Zhang J, Wu X, Gong Q (2009) Resonant Modes of L-Shaped Gold Nanoparticle. *Chinese Phys Lett* 26:067802
- Elghanian R, Storhoff JJ, Mucic RC, Letsinger RL, Mirkin CA (1997) Selective Colorimetric Detection of Polynucleotides Based on the Distance-Dependent Optical Properties of Gold Nanoparticles. *Science* 277:1078–1081
- Haes AJ, Chang L, Klein WL, Duyne RPV (2005) Detection of a Biomarker for Alzheimer’s Disease from Synthetic and Clinical Samples Using a Nanoscale Optical Biosensor. *J Am Chem Soc* 127:2264–2271
- Hohenau A, Krenn JR, Beermann J, Bozhevolnyi SI, Rodrigo SG, Martin-Moreno L, Garcia-Vidal F (2006) Spectroscopy and nonlinear microscopy of Au nanoparticle arrays: experiment and theory. *Phys Rev B* 73:155404
- Hohenau A, Krenn JR, Garcia-Vidal FJ, Rodrigo SG, Martin-Moreno L, Beermann J, Bozhevolnyi SI (2007) Spectroscopy and nonlinear microscopy of gold nanoparticle arrays on gold films. *Phys Rev B* 75:085104
- Cubukcu E, Kort EA, Crozier KB, Capasso F (2006) Plasmonic laser antenna. *Appl Phys Lett* 89:093120
- Yang J, Zhang J (2011) Subwavelength Quarter-Waveplate Composed of L-Shaped Metal Nanoparticles. *Plasmonics*. doi:10.1007/s11468-010-9196-x
- Muskens OL, Giannini V, Sánchez-Gil JA, Rivas JG (2007) Strong Enhancement of the Radiative Decay Rate of Emitters by Single Plasmonic Nanoantennas. *Nano Lett* 7:2871–2875
- Veronis G, Fan S (2007) Modes of Subwavelength Plasmonic Slot Waveguides. *J Lightwave Technol* 25:2511–2521
- Veronis G, Fan S (2005) Guided subwavelength plasmonic mode supported by a slot in a thin metal film. *Opt Lett* 30:3359–3361
- Pile DFP, Ogawa T, Gramotnev DK, Matsuzaki Y, Vernon KC, Yamaguchi K, Okamoto T, Haraguchi M, Fukui M (2005) Two-dimensionally localized modes of a nanoscale gap plasmon waveguide. *Appl Phys Lett* 87:261114
- Lynch DW, Hunter WR (1985) Gold (Au). In: Palik ED (ed) *Handbook of Optical Constants of Solids*. Academic, Orlando, pp 286–295
- Wu X, Zhang J, Gong Q (2009) Metal-insulator-metal nanorod arrays for subwavelength imaging. *Opt Express* 17:2818–2825